IEEE Access
Multidisciplinary | Rapid Review | Open Access Journal

Received 13 December 2023, accepted 23 December 2023, date of publication 27 December 2023,
date of current version 3 January 2024.

Digital Object Identifier 10.1109/ACCESS.2023.3347611

RESEARCH ARTICLE

L2-SSA-LSTM Prediction Model of Steering Drilling Wellbore Trajectory

YI GAO[1,2], NA WANG[1], AND YIHAO MA[1]
[1]School of Electronic Engineering, Xi'an Shiyou University, Xi'an, Shaanxi 710065, China
[2]Key Laboratory of Measurement and Control Technology for Oil and Gas Wells, Xi'an Shiyou University, Xi'an, Shaanxi 710065, China

Corresponding author: Yi Gao (gy@xsyu.edu.cn)

This work was supported in part by the National Natural Science Foundation of China under Grant 51604226, and in part by the Shaanxi Natural Science Basic Research Project 2023-JC-YB-453.

ABSTRACT The high-speed vibration rotation of the drill bit during drilling causes the logging tool to be damaged or distorted, resulting in inaccurate or lost data collection. Traditional prediction methods such as dynamic modeling and geological modeling have problems such as incomplete data and difficult modeling, which cannot meet the accuracy and stability requirements of wellbore trajectory prediction. The long short-term memory neural network (LSTM) for predicting time series can achieve accurate prediction, but there are problems such as difficulty in adjusting the hyperparameters of the LSTM model, slow convergence speed, and easy overfitting. This paper absorbs the advantages of the LSTM algorithm, ridge regression (L2 regularization), and sparrow optimization algorithm (SSA) in machine learning and proposes a well trajectory prediction model of steerable drilling based on L2 regularization and SSA optimized LSTM (L2-SSA-LSTM). The model takes the LSTM hyperparameter as the parameter optimization goal of SSA and adds L2 regularization to the model to prevent model overfitting to complete modeling and prediction. The experiment was conducted using measured data sets from directional drilling in two different oilfields. The results show that compared with the back propagation algorithm (BP), consolidated memory gated recurrent unit (CMGRU), dual-thread gated recurrent unit (DTGRU), Attention-based Spatiotemporal Graph Recurrent Neural Network (ASTG-RNN), LSTM, and the L2-SSA-LSTM prediction model has significantly higher accuracy in predicting directional drilling trajectories than other models and has the better predictive ability.

INDEX TERMS Steering drilling system, wellbore trajectory prediction, long short-term memory neural network, sparrow optimization algorithm, L2 regularization.

I. INTRODUCTION

Drilling engineering has always been one of the essential tasks in the oil and gas industry. To extract oil and gas resources more effectively, precise control of the wellbore trajectory is necessary [1]. Accurate prediction of the wellbore trajectory contributes to efficient resource extraction, reduces the impact on the surface environment, ensures the safety of workers, and maximizes resource recovery [2], [3]. Wellbore trajectory prediction is not just an engineering challenge, it is a comprehensive consideration involving efficiency, sustainability, and safety. By continuously improving and optimizing wellbore trajectory prediction techniques, the oil and gas industry can ensure the success and sustainability of drilling operations [4], [5], [6]. Therefore, accurate wellbore trajectory prediction is of paramount importance in petroleum extraction.

Wellbore trajectory prediction refers to judging the extension direction of the wellbore according to the current trend of the wellbore. Wellbore trajectory prediction plays an important role in oil drilling, and scholars at home and abroad are also committed to research in this field. Li et al. used the transfer matrix principle to model the lateral force at the drill bit in a complex BHA. After obtaining the lateral

The associate editor coordinating the review of this manuscript and approving it for publication was Alberto Cano.

force and weight on the bit bottom hole assembly (WOB), they considered drilling conditions to assess the expected bit direction for wellbore trajectory prediction [7]. This method did not account for practical considerations and was suitable primarily for theoretical calculations. Yang et al. addressed the aforementioned issue by proposing a longitudinal, torsional, and radial-coupled drill string dynamic model. They obtained parameters such as the torsional angle displacement and angular velocity during normal drilling and stick-slip vibration phases for trajectory prediction [8]. This approach considered various factors during normal drilling and stick-slip vibration phases, but the influence of drill bit noise resulted in suboptimal predictive performance. Xie et al, based on a statistical analysis of the wellbore trajectory data from horizontal sections drilled in Jiangsu Oilfield, established a sine trigonometric function model for horizontal wellbore trajectory prediction [9]. This method could predict wellbore trajectories relatively easily based on known data from horizontal sections with similar geological conditions. However, its predictive performance was not ideal for different geological environments and wellbore types. Samuel et al. introduced a coupled model embedded with uncertainty by combining geometry, BHA dynamics, and dynamic earth models. This integrated various models and factors to achieve more accurate wellbore trajectory prediction [10]. However, the complexity of the model and consideration of multiple factors might increase computational complexity, necessitating more computing resources and time. Yan et al. proposed using the random forest method for predicting azimuth, deviation angle, and tool face angle [11]. This approach only required data-based wellbore trajectory prediction without the need for complex models. However, random forests cannot capture the temporal correlations and dynamics of sequential data, making them less suitable for time series data. Furthermore, the model parameters are not easily adjustable.

To improve the prediction performance, Liu et al. proposed an interactive ship trajectory prediction framework based on LSTM (QSD-LSTM), which is beneficial for avoiding unnecessary collisions between adjacent ships [12]. Hasan et al. proposed a multi-head attention-based LSTM sequence model for modeling social and temporal interactions and predicting the future trajectories of surrounding vehicles [13]. Wang presented a novel off-road multi-agent trajectory prediction framework called SA-LSTM for predicting autonomous off-road vehicle trajectories [14]. Zhang et al. proposed a time-aware LSTM single-ship trajectory model in combination with a Generative Adversarial Network (GAN) to predict the trajectories of multiple ships [15]. To accurately predict high-precision cutter head torque (CHT), Qin et al. proposed a new embedded long short-term memory (ELSTM) network with a dual memory structure [16]. To improve the ability to predict complex degradation trajectories, Zhou et al. studied a new Dual-Thread Gated Recurrent Unit (DTGRU) to predict the remaining useful life and provide a basis for the operation and maintenance of industrial equipment. At the same time, in the face of the gap in unsupervised construction of health index (HI) with a unified fault threshold, they combined the proposed distributed contact ratio metric health index (DCRHI) with the integrated memory gated cycle unit (CMGRU) to propose a novel remaining useful life (RUL) prediction method to improve the prediction performance [17], [18].

While LSTM has been widely applied in trajectory prediction fields, its use in wellbore trajectory prediction is limited. Only Meng et al. presented a new prediction model based on LSTM networks, which predicts the deviation and azimuth angles through LSTM modeling [19]. Although their method does not rely on assumptions about path shapes or geometries and solely depends on past data, the model is prone to overfitting, challenging parameter adjustments, and involves long execution times and high computational costs.

Based on the aforementioned research, traditional methods for predicting wellbore trajectory are limited when dealing with complex geological conditions, making it challenging to accurately forecast wellbore trajectories. Furthermore, the existing wellbore trajectory prediction algorithm will have problems such as difficulty in super-parameter adjustment and easy over-fitting. Given the above problems, this paper proposes an L2-SSA-LSTM prediction model for steering drilling wellbore trajectory by combining L2 regularization, SSA, and LSTM. The SSA technique is utilized to search for the optimal hyperparameter combination for LSTM, while L2 regularization aids in preventing overfitting in the model. The model automatically optimizes the parameters of the LSTM network, capturing long-term dependencies, thereby improving prediction accuracy and generalization capability. It applies to various types of wellbore trajectory data. Through simulation experiments, the prediction results of BP, CMGRU, DTGRU, ASTG-RNN, and LSTM models are compared and analyzed. It is proved that the method has high prediction accuracy, can effectively improve drilling efficiency, and reduces drilling costs.

II. THEORETICAL BASIS

A. LONG SHORT-TERM MEMORY NETWORK(LSTM)

LSTM neural network is an RNN (Recurrent Neural Network) aimed at solving the problem of gradient explosion and vanishing that often occur during long-term sequence training [20], [21]. They are particularly well-suited for handling time series data [22], [23]. LSTM networks are governed by the presence of a forget gate, input gate, and output gate, which collectively control the cell state, the overall structure is shown in Figure 1 and the calculation for the three gates is as follows:

$$\boldsymbol{f_t} = \sigma(\boldsymbol{W_f} \cdot [h_{t-1}, x_t] + \boldsymbol{b_f}) \tag{1}$$

$$\sigma(x) = \frac{1}{1 + e^{-x}} \tag{2}$$

$$\boldsymbol{i_t} = \sigma(\boldsymbol{W_i} \cdot [h_{t-1}, x_t] + \boldsymbol{b_i}) \tag{3}$$

$$\widetilde{C}_t = tanh(W_c \cdot [h_{t-1}, x_t] + b_c) \tag{4}$$

$$C_t = f_t * C_{t-1} + i_t * \widetilde{C}_t \tag{5}$$

$$tanh(x) = \frac{e^x - e^{-x}}{e^x + e^{-x}} \tag{6}$$

$$O_t = \sigma(W_o \cdot [h_{t-1}, x_t] + b_o) \tag{7}$$

$$h_t = O_t * tanh(C_t) \tag{8}$$

where x_t is the input information at time t; h_{t-1}represents the previous hidden state; h_t is hidden state at the next moment; W_f, W_i, W_c, W_o is the weight matrix; b_f, b_i, b_c, b_o is the bias vector; f_t is the forgetting gate; i_t is the input gate; O_t is the output gate; $\widetilde{C}_t$ is candidate cell states; C_t is the new cell state; C_{t-1} represents the cell state at the previous moment; $\sigma(x)$ and $tanh(x)$ is the activation function.

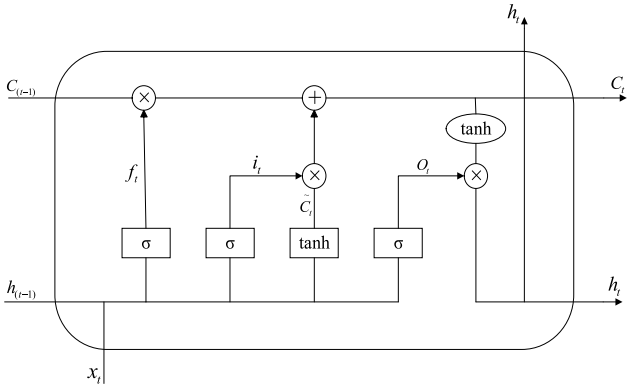

FIGURE 1. The overall structure of the LSTM neural network.

B. SPARROW OPTIMIZATION ALGORITHM(SSA)

The Sparrow algorithm is a novel intelligent optimization algorithm based on the foraging and anti-predation behavior of sparrow populations, with the ability to globally search and develop locally [24], [25]. During each iteration, location updates for discoverers, entrants, and sparrows who are aware of the danger are as follows:

$$X_{i,j}^{t+1} = \begin{cases} X_{i,j}^{t} \cdot exp(-\dfrac{i}{\alpha \cdot item_{max}}) & if\ R_2 < ST \\ X_{i,j}^{t} + Q \cdot L & if\ R_2 > ST \end{cases} \tag{9}$$

$$X_{i,j}^{t+1} = \begin{cases} Q \cdot exp(-\dfrac{X_{worse} - X_{i,j}^{t}}{i^2}) & if\ i > n/2 \\ X_P^{t+1} + \left| X_{i,j} - X_P^{t+1} \right| \cdot A^{+} \cdot L & others \end{cases} \tag{10}$$

$$X_{i,j}^{t+1} = \begin{cases} X_{best}^{t} + \beta \cdot \left| X_{i,j}^{t} - X_{best}^{t} \right| & if\ f_i < f_g \\ X_{i,j}^{t} + K \cdot (\dfrac{\left| X_{i,j}^{t} - X_{worst}^{t} \right|}{(f_g - f_\omega) + \varepsilon}) & if\ f_i > f_g \end{cases} \tag{11}$$

where $item_{max}$ is a constant representing the maximum number of iterations; $X_{i,j}$ indicates the information position of the $i-th$ sparrow in the $j-th$ dimension; α is a random number; R_2 and ST represent warning and safety thresholds; Q is a random number; L denotes a matrix; X_P represents the current best position occupied by the discoverer; X_{worst} denotes the current worst global position; A represents a matrix; $A^+$is a constant; X_{best} represents the global best position; β is a step size control parameter; K is a random number; f_g and f_ω represent the global best and worst fitness values; ε is an extremely small constant.

III. L2-SSA-LSTM PREDICTION MODEL

A. LSTM NETWORK OPTIMIZATION

Because the LSTM model takes into account the dependencies between continuous events and possesses a unique memory structure with long-term memory capabilities, it is highly suitable for addressing problems highly correlated with time series [26]. Therefore, for the real-time mutations in wellbore trajectory data and their time dependence, the LSTM model was chosen as the fundamental prediction model for wellbore trajectory forecasting. However, LSTM networks are prone to issues such as overfitting.

Common methods to prevent model overfitting include discarding, stopping training in advance, ensemble learning, batch standardization, and maximum norm constraint, but there are some shortcomings when applied to the LSTM network. For the training data set, the discarding method randomly closes the unit during training, which will affect the memory performance of LSTM. The early stop training method makes it difficult to stop training at the right time, and a large part may prematurely terminate the learning of the model, resulting in the model failing to fully fit the training data; the ensemble learning method integrates multiple LSTM models to increase the computational complexity; for cyclic structures such as LSTM, the maximum norm constraint may not be easy to implement or need to be carefully adjusted. The L2 regularization actually imposes a constraint on the weight by adding the quadratic sum penalty term of the weight to the loss function. This helps to limit the size of the weight and prevent its excessive growth, thereby slowing down the model's overfitting of the training data. In addition, the use of L2 regularization helps to improve the generalization ability and robustness of the model.

In the LSTM network, L2 regularization limits the size of the model parameters by adding a penalty term for the sum of squares of the weight matrix to the loss function, thereby reducing the complexity of the model and preventing it from overfitting the training data. By setting the hyperparameters of the LSTM network, the L2 regularization term is added to the weight matrix. During the training process, the optimizer not only updates the model parameters to reduce the original loss function but also updates the L2 regularization term by gradient descent. The weight update process is as follows:

The LSTM network is optimized by L2 regularization, and the formula of the loss function L is as follows:

$$L = L_0 + \frac{\lambda}{2} \parallel \omega \parallel^2 = L_0 + \frac{\lambda}{2} \omega^{\mathrm{T}} \omega \tag{12}$$

where $\boldsymbol{L_0}$ represents the model's average loss, $\boldsymbol{\omega}$ signifies the L2 norm of the parameter vector, and λ serves as a hyperparameter that controls the strength of L2 regularization.

The corresponding gradient is:

$$\frac{\partial \boldsymbol{L}}{\partial \boldsymbol{\omega}} = \frac{\partial \boldsymbol{L_0}}{\partial \boldsymbol{\omega}} + \lambda \boldsymbol{\omega} \tag{13}$$

Based on equations (12) and (13), the update for the weight ω is as follows:

$$\boldsymbol{\omega} \rightarrow \boldsymbol{\omega} - \eta \left(\frac{\partial \boldsymbol{L_0}}{\partial \boldsymbol{\omega}} + \lambda \boldsymbol{\omega} \right) = (1 - \eta\lambda)\, \boldsymbol{\omega} - \eta \frac{\partial \boldsymbol{L_0}}{\partial \boldsymbol{\omega}} \tag{14}$$

where η is the learning rate.

Therefore, the weight update formula for L2-regularized LSTM can be expressed as:

$$\boldsymbol{W_f}\,(k+1) = \boldsymbol{W_f}\,(k) - \eta \frac{\partial \boldsymbol{L}}{\partial \boldsymbol{W_f}\,(k)} \tag{15}$$

where $\boldsymbol{W_f}$ represents the weight of the forget gate, and k stands for the time step.

The updated formulas for the remaining weights are similar.

B. LSTM NETWORK HYPERPARAMETER OPTIMIZATION

The selection of hyperparameters for the LSTM model has a significant impact on the model's prediction accuracy. Typically, empirical methods are used to choose hyperparameters, but this approach is arbitrary and blind, lacking universality and failing to achieve optimal predictive results [27]. Therefore, the SSA is employed to perform a hyperparameter search for the LSTM model. It maps multiple hyperparameters into a multidimensional space, using root mean square error as the fitness function to find the information corresponding to the optimal value for obtaining the best hyperparameter combination. This reduces the randomness and blindness in hyperparameter selection.

The LSTM model has many hyperparameters. SSA is used to dynamically optimize the four key parameters in the network model: LSTM hidden layer number, training iteration number, maximum batch size, and learning rate. At the same time, the L2 regularization coefficient is optimized to find the best hyperparameter combination to achieve the optimal state of the network. Firstly, the optimization range of each hyperparameter is determined. Secondly, a group of sparrow individuals are randomly generated, and each individual corresponds to a set of hyperparameters. At the same time, the sparrow group is allowed to explore within the range of hyperparameters, and information is shared among individuals. Then, RMSE is selected as the loss function to evaluate the performance of the model. Then use Equations (9), (10), (11) to continuously update the position of the sparrow and calculate the fitness; finally, a combination of hyper-parameters with good performance is output, and this combination is used to train and predict the network. The steps and process of the L2-SSA-LSTM prediction model are illustrated in Figure 2 as follows:

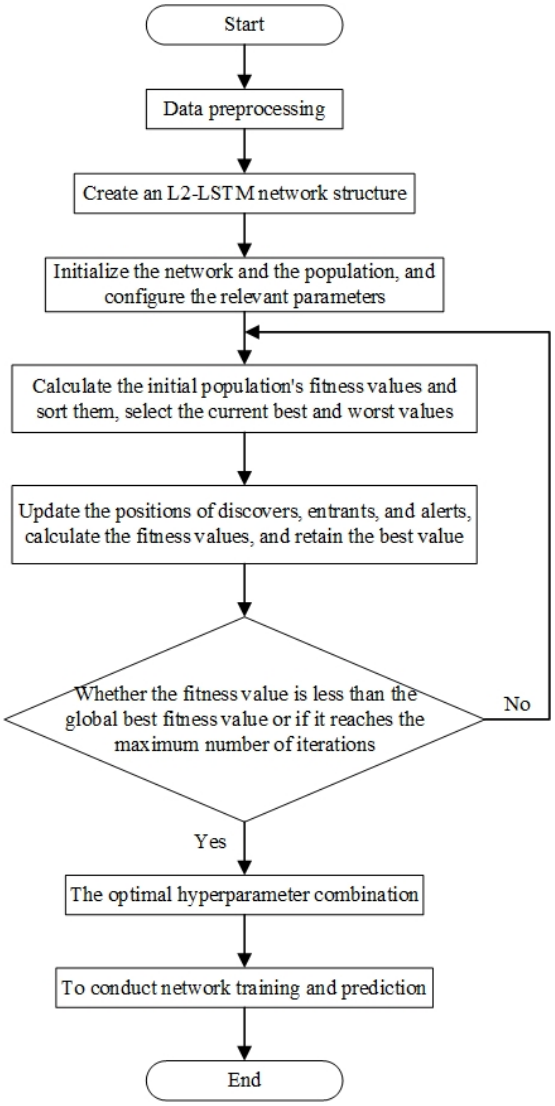

FIGURE 2. The overall structure of the system model.

Step1 Data Preprocessing: Normalize the data and split the dataset into training and testing sets based on a certain ratio.

Step2 Establish Network Structure: Optimize the LSTM network using L2 regularization to prevent network overfitting by updating the weight values.

Step3 Initialization: Initialize the network and the sparrow population, define parameters related to the sparrow search algorithm, and set the maximum number of iterations.

Step4 Select the root mean square error as the fitness value, calculate the fitness values of the initial population, and sort them to select the current best and worst values.

Step5 Real-time updates the positions of sparrow finders, joiners, and sentinels, calculate the fitness values of the sparrow population, and retain the best positions of individuals in the population.

Step6 Determine whether the condition of being less than the global best fitness value or reaching the maximum

number of iterations is met. If satisfied, obtain the optimized parameters. otherwise, continue with Steps 4 to 5.

Step7 The final value output by the Sparrow Search Algorithm is considered the best hyperparameter combination.

Step8 Train the LSTM network using the best hyperparameter combination and proceed with predictions.

IV. SIMULATION EXPERIMENTS AND ANALYSIS

A. DATA PREPROCESSING

Trajectory prediction methods can be mainly divided into physical modeling prediction and data-driven non-physical model prediction. In this paper, the data-driven non-physical model prediction method is used to transform the wellbore trajectory prediction problem into a time series prediction problem. Through the analysis and identification of historical time series data, we extract drilling bit motion information contained in historical wellbore trajectories, thereby avoiding the complexities of modeling and computations. Because this method relies solely on data, the selection of feature data is crucial.

To achieve the ideal stratum, through the guidance control and its positioning in the underground space, to ensure the accurate positioning of the stratum. The measured values collected by the sensors, including azimuth angle, deviation angle, and tool face angle, offer critical information about the spatial position and orientation of the wellbore in the subsurface. The azimuth angle helps determine the wellbore's orientation relative to the geographic coordinate system. The deviation angle of the wellbore dictates its depth and position in the underground space. The tool face angle of the wellbore allows for adjustments in the drill bit's direction to ensure that the wellbore progresses in the desired direction. Therefore, in the prediction of wellbore trajectories, forecasting the azimuth angle, deviation angle, and tool face angle is crucial for predicting the path of the wellbore. So, choose these three feature datasets to serve as the dataset for our prediction model.

Before inputting the dataset into the LSTM model, data preprocessing is essential to ensure the reliability and accuracy of the analysis. In this paper, we employ interpolation to estimate missing values, preserving data integrity, and preventing data loss. We replace outliers with the average of the surrounding ten data points, reducing the impact of outliers with the data and mitigating noise and fluctuations. Subsequently, we normalize the data, bringing all values into roughly the same numerical range, thereby eliminating dependency on measurement units, and improving model performance. This aids in model training and accelerates model convergence. The formulas for outlier handling and normalization are given by Equation (16) and Equation (17), respectively:

$$\bar{z} = \frac{z_{i-10} + \cdots + z_{i-1} + z_{i+1} + \ldots + z_{i+10}}{20} \tag{16}$$

$$x_i' = \frac{x_i - \bar{x}}{\frac{1}{n}\sum_{i=1}^{1}(x_i - \bar{x})}, i = 1, 2, 3, \cdots \tag{17}$$

where i represents the order of the existence of outliers, z_i denotes outliers, and $\bar{z}$ stands for the mean value. x_i' is the normalized data value; x_i is the sample value; $\bar{x}$ is the mean value of the sample; $n$is the total number.

B. EVALUATION METRICS

To provide a more comprehensive evaluation of the forecasting performance of different methods and to overcome the limitations of a single evaluation metric, we chose to utilize three evaluation criteria to assess the performance of our algorithm models, namely the Root Mean Squared Error (RMSE), Mean Absolute Percentage Error (MAPE), and Coefficient of Determination (R^2). The formulas for each evaluation metric are as follows:

$$RMSE = \sqrt{\frac{\sum_{i=1}^{n}\left(\hat{y}_i - y_i\right)^2}{n}} \tag{18}$$

$$MAPE = \frac{1}{n}\sum_{i=1}^{n}\left|\frac{\hat{y}_i - y_i}{y_i}\right| \times 100\% \tag{19}$$

$$R^2 = 1 - \frac{\sum_{i=1}^{n}\left(y_i - \hat{y}_i\right)^2}{\sum_{i=1}^{n}\left(y_i - \bar{y}_i\right)^2} \tag{20}$$

where n is the number of predicted samples, y_i represents the observed values. $\hat{y}_i$ represents the predict values. The smaller the values of RMSE and MAPE evaluation metrics, the better the predictive performance of the model. The closer the R^2 evaluation metric is to 1, the better the model's performance.

C. DETERMINATION OF MODEL PARAMETERS

Because the model predicts the three-time series data of azimuth angle, deviation angle, and tool face angle respectively, the LSTM model sets the input layer and the fully connected layer to 1; through the cross-validation method, the threshold is set to 1, the learning rate drop factor is set to 0.1, and the number of times is set to 300 under the learning rate; At the same time, in order to find the appropriate number of hidden layer neurons, the number of iterations, the number of samples included in each training, the learning rate and the regularization coefficient, the sparrow algorithm is used to optimize these hyperparameters. According to the experience, the number of sparrow populations is set to 20, the proportion of sparrow producers is set to 20%, and the number of iterations of the search algorithm is set to 100. Since the optimized parameters are the number of hidden layer neurons, the number of iterations, the number of samples included in each training, the learning rate, and the regularization coefficient, the descending optimization dimension is set to 5. According to the experience, the initial range of sparrow position is set to the number of hidden layer neurons [8,64], the number of iterations [500,1500], the number of samples included in each training [16,64], the learning rate [0.001,0.1], the regularization coefficient [0,0.01].

D. CASE STUDY

All experimental simulation platforms are MATLAB 2019b.

After obtaining experimental data and preprocessing, the BP neural network model, CMGRU neural network model, DTGRU neural network model, ASTG-RNN neural network model, LSTM neural network model, and L2-SSA-LSTM neural network model are used to compare and analyze the results. The effectiveness of the proposed method is verified by comparing the error evaluation indexes and prediction accuracy of different neural network models.

Case 1:

The data used in this example was obtained from the measured wellbore trajectory data in a certain oilfield in Jilin Province. The azimuth angle, deviation angle, and tool face angle data were collected from 0 meters to 2760 meters using Measurement While Drilling (MWD), with a data sampling interval of 5 seconds. The sample data is divided into a training set and a test set, with 90% of the data used for training and 10% for testing. The constructed model was implemented through computer programming, and experimental validation was performed separately for azimuth angle, deviation angle, and tool face angle.

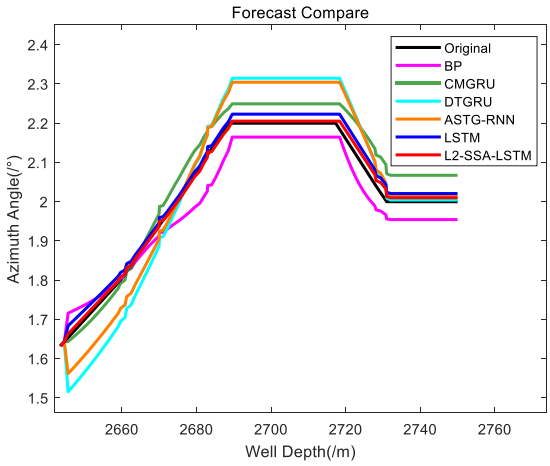

FIGURE 3. Azimuth angle prediction results of various models.

TABLE 1. Prediction error of different azimuth angle models.

Prediction Model	R^2	RMSE	MAPE
BP	0.91585	0.04667	0.00176
CMGRU	0.88647	0.05421	0.02245
DTGRU	0.69446	0.08893	0.01331
ASTG-RNN	0.78271	0.07501	0.01643
LSTM	0.98091	0.02223	0.00995
L2-SSA-LSTM	0.99576	0.01047	0.00306

1) AZIMUTH ANGLE PREDICTION

From Figure 3, it can be observed that among the azimuth angle prediction models, including BP, CMGRU, DTGRU, ASTG-RNN, LSTM, and L2-SSA-LSTM, the L2-SSA-LSTM model exhibits superior predictive performance compared to the others. According to Figure 4, the DTGRU and ASTG-RNN neural network prediction models exhibit relatively large errors, resulting in less-than-ideal predictions and an inability to achieve the desired prediction accuracy. In comparison to these two neural network prediction models, the errors generated by CMGRU and BP neural network prediction models are reduced, and their prediction accuracy is relatively high, although they still operate at a relatively elevated error level. The LSTM neural network prediction model generates smaller errors than CMGRU and BP neural network prediction models, but its prediction accuracy remains relatively high without reaching the desired level. The L2-SSA-LSTM neural network prediction model achieves excellent predictions for the majority of sampling points, demonstrating minimal prediction errors and significantly improved prediction accuracy.

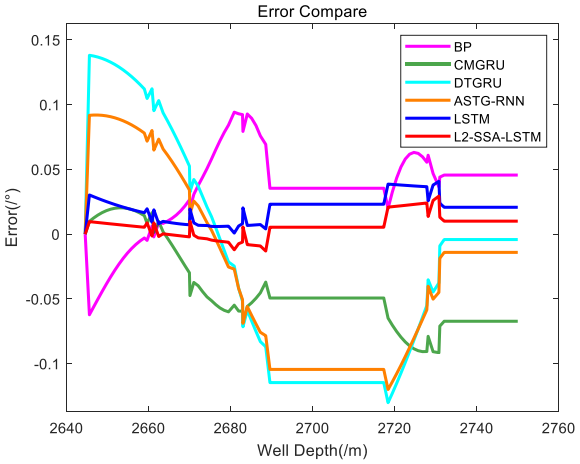

FIGURE 4. Prediction error results of various models.

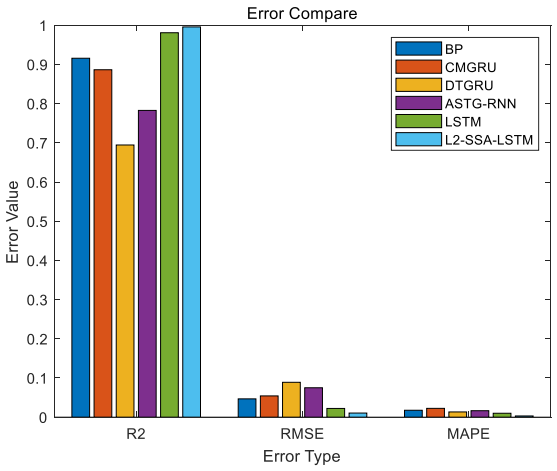

FIGURE 5. Comparison of evaluation metrics.

As evident from Table 1 and Figure 5, the prediction accuracy of the L2-SSA-LSTM neural network model is notably higher than that of other prediction models, with R^2, RMSE, and MAPE values of 0.99576, 0.01047, and 0.00306,

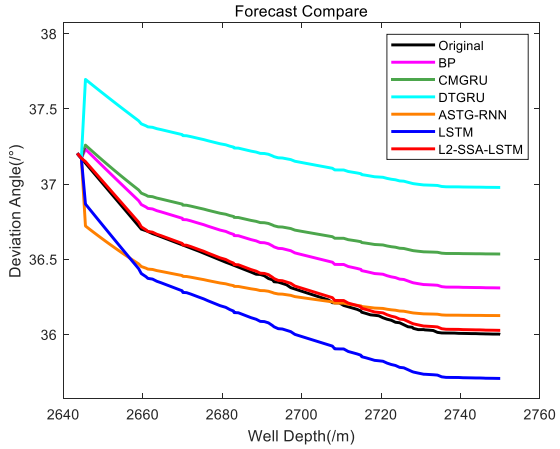

FIGURE 6. Deviation angle prediction results of various models.

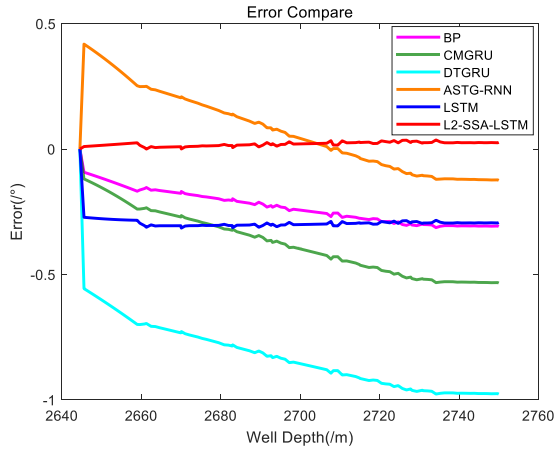

FIGURE 7. Prediction error results of various models.

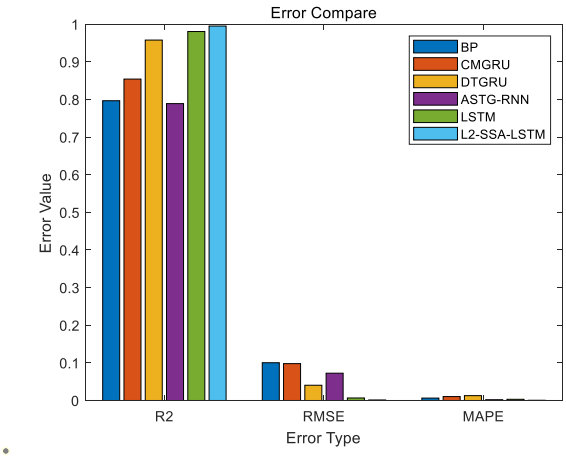

FIGURE 8. Comparison of evaluation metrics.

respectively. In comparison to other neural network prediction models, each evaluation metric has decreased, indicating that the L2-SSA-LSTM neural network prediction model possesses higher predictive accuracy. It excels in predicting the azimuth angle of the wellbore trajectory.

TABLE 2. Prediction error of different deviation angle models.

Prediction Model	R^2	RMSE	MAPE
BP	0.79668	0.10033	0.00637
CMGRU	0.85429	0.09796	0.01038
DTGRU	0.95794	0.04052	0.01285
ASTG-RNN	0.78904	0.07254	0.00197
LSTM	0.98068	0.00667	0.00315
L2-SSA-LSTM	0.99524	0.00134	0.00054

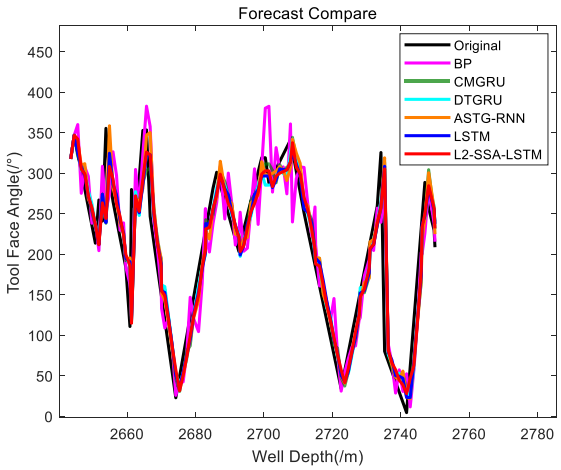

FIGURE 9. Tool face angle prediction results of various models.

2) DEVIATION ANGLE PREDICTION

From Figures 6 and 7, it can be roughly observed that, for the prediction of wellbore deviation angles, the dual linear learning strategy in DTGRU captures the correlation between individual data and its historical data slightly less effectively than LSTM. As a result, the predictive performance of DTGRU is relatively poor. While LSTM and CMGRU neural network models outperform DTGRU in predicting deviation angles, the errors in the prediction results are still relatively large. This may be attributed to LSTM not tuning to appropriate hyperparameters and DTGRU's inability to capture longer-range dependencies as effectively as LSTM. Therefore, the predictive accuracy remains unsatisfactory. Both BP and ASTG-RNN neural network models yield better prediction results than LSTM, but the prediction errors in wellbore deviation angles are still relatively high, falling short of the desired precision. The L2-SSA-LSTM model demonstrates good predictive performance for the majority of wellbore deviation angle samples. The prediction errors are smaller compared to other models, and the accuracy aligns with the expected precision.

Table 2 and Figure 8 indicate that the evaluation metrics RMSE, MAPE, and R^2 for the L2-SSA-LSTM neural network prediction model are 0.00134, 0.00054, and 0.99524, respectively. In comparison to other models, the predictive accuracy of the L2-SSA-LSTM neural network model is significantly improved, with each evaluation metric showing

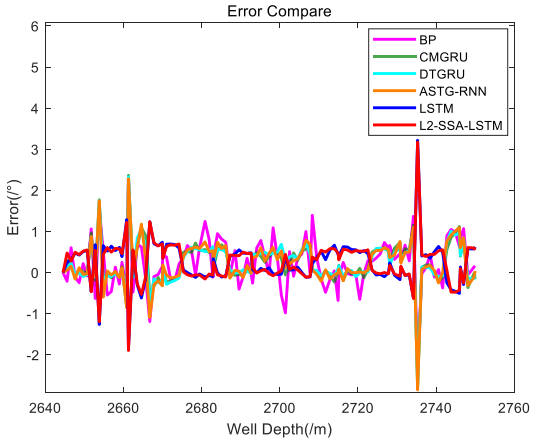

FIGURE 10. Prediction error results of various models.

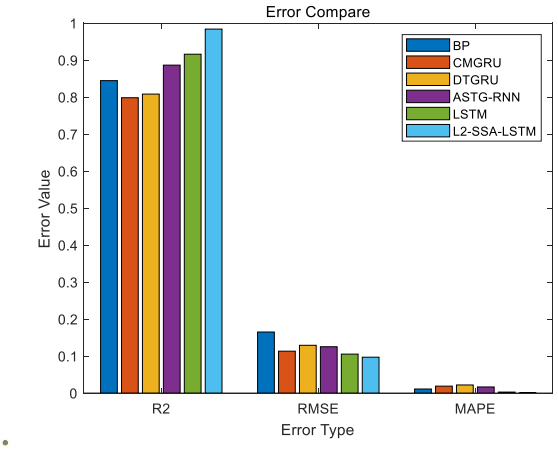

FIGURE 11. Comparison of evaluation metrics.

TABLE 3. Prediction error of different tool face angle models.

Prediction Model	R^2	RMSE	MAPE
BP	0.84438	0.16496	0.01093
CMGRU	0.79822	0.11315	0.01868
DTGRU	0.80806	0.12907	0.02183
ASTG-RNN	0.88633	0.12514	0.01646
LSTM	0.91583	0.10523	0.00261
L2-SSA-LSTM	0.98374	0.09689	0.00025

a decrease. This suggests that the LSTM model optimized through SSA and L2 regularization has better predictive accuracy and stronger applicability for wellbore trajectory deviation angles.

3) TOOL FACE ANGLE PREDICTION

By comparing Figure 9 and Figure 10, it can be observed that six models, namely BP, CMGRU, DTGRU, ASTG-RNN, LSTM, and L2-SSA-LSTM, are employed to predict the tool face angle of wellbore trajectory. The prediction errors of the BP neural network model are relatively large, and the

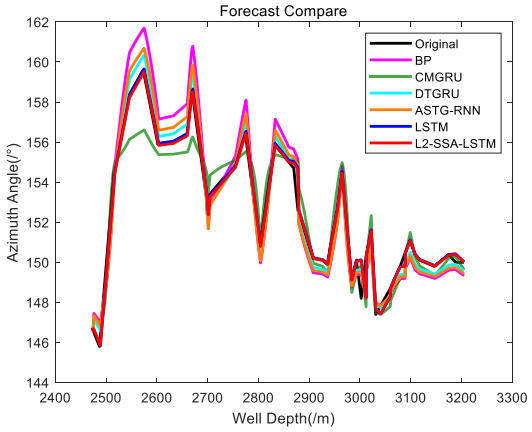

FIGURE 12. Azimuth angle prediction results of various models.

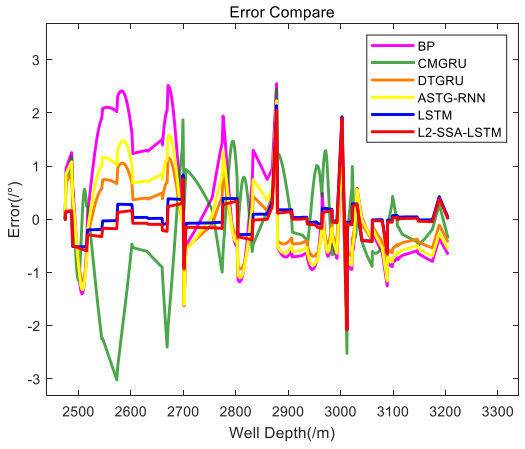

FIGURE 13. Prediction error results of various models.

prediction accuracy does not reach the desired level, indicating poor performance. In comparison to the BP neural network model, the prediction errors of the CMGRU, DTGRU, and ASTG-RNN models are reduced, but their prediction accuracy is relatively poor and falls short of the desired effectiveness. The LSTM neural network model exhibits reduced prediction errors compared to CMGRU, DTGRU, and ASTG-RNN, but the errors remain relatively high, indicating suboptimal prediction accuracy. The L2-SSA-LSTM model demonstrates good prediction performance for the majority of sampling points, with small prediction errors and significantly improved accuracy.

Through Table 3 and Figure 11, it can be seen that, in the prediction of tool face angle, the evaluation metrics RMSE, MAPE, and R^2 for the L2-SSA-LSTM model are 0.02599, 0.01218, and 0.99917, respectively. Compared to various evaluation metrics of other models, the predictive accuracy of the L2-SSA-LSTM model is significantly higher, enhancing the precision of predicting the tool face angle of wellbore trajectory and demonstrating strong applicability.

Case 2:

The data used in the second example of this paper is obtained from the measured wellbore trajectory data in a

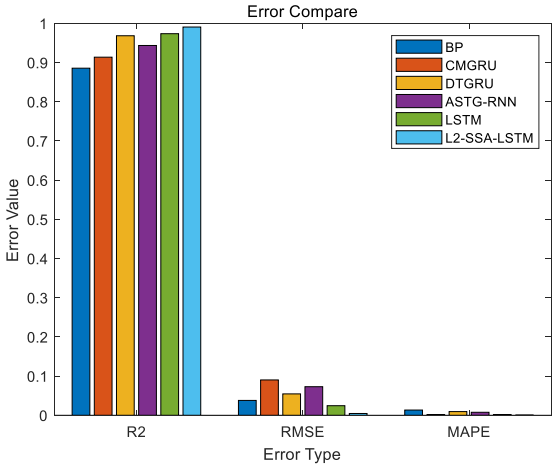

FIGURE 14. Prediction error results of various models.

TABLE 4. Prediction error of different azimuth angle models.

Prediction Model	R^2	RMSE	MAPE
BP	0.88565	0.03791	0.01333
CMGRU	0.91374	0.09015	0.00146
DTGRU	0.96842	0.05454	0.00938
ASTG-RNN	0.94359	0.07288	0.00762
LSTM	0.97367	0.02441	0.00157
L2-SSA-LSTM	0.99065	0.00456	0.00039

certain oilfield in Fuyu, Jilin Province. The azimuth angle, deviation angle, and tool face angle data were collected from 0 meters to 3205 meters using MWD, with a data sampling interval of 10 seconds. The sample data is divided into a training set and a test set, with 90% of the data used for training and 10% for testing. The constructed model was implemented through computer programming, and experimental validation was performed separately for azimuth angle, deviation angle, and tool face angle.

4) AZIMUTH ANGLE PREDICTION

From Figure 12 and Figure 13, it can be observed that the predictive performance of the LSTM and L2-SSA-LSTM models in azimuth angle prediction is better than that of other models. This is mainly because the LSTM model, compared to BP and ASTG-RNN models, can better capture the historical data of azimuth angles, resulting in a more effective prediction. On the other hand, LSTM, with its three gates, is more flexible and powerful than CMGRU and DTGRU, exhibiting better expressive capability and improved azimuth angle prediction performance. The superior performance of the L2-SSA-LSTM model compared to LSTM can be attributed to the self-selection of the L2 regularization coefficient, avoiding potential overfitting issues associated with a too-high coefficient. Additionally, in the L2-SSA-LSTM model, SSA can automatically find the optimal hyperparameters, addressing the difficulty of hyperparameter tuning and further enhancing azimuth angle prediction.

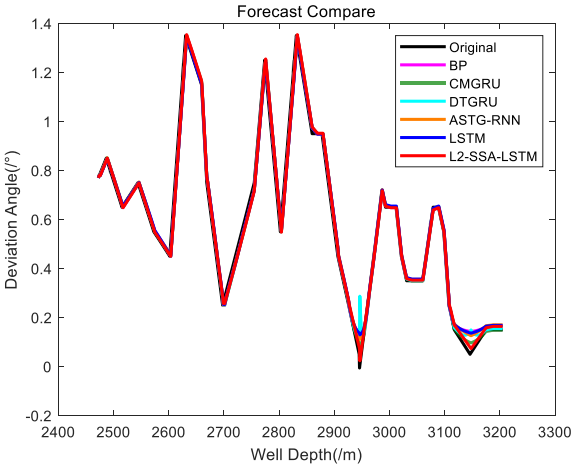

FIGURE 15. Deviation angle prediction results of various models.

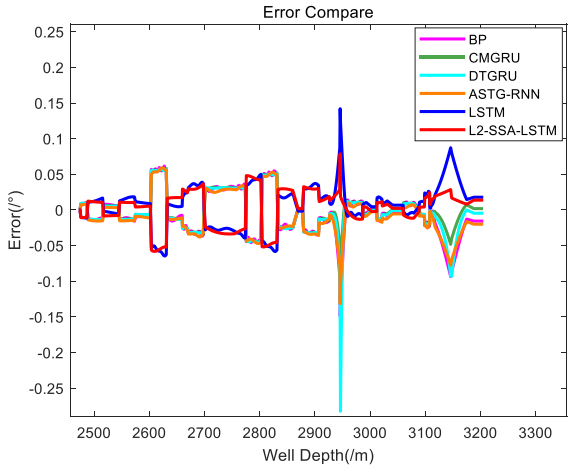

FIGURE 16. Prediction error results of various models.

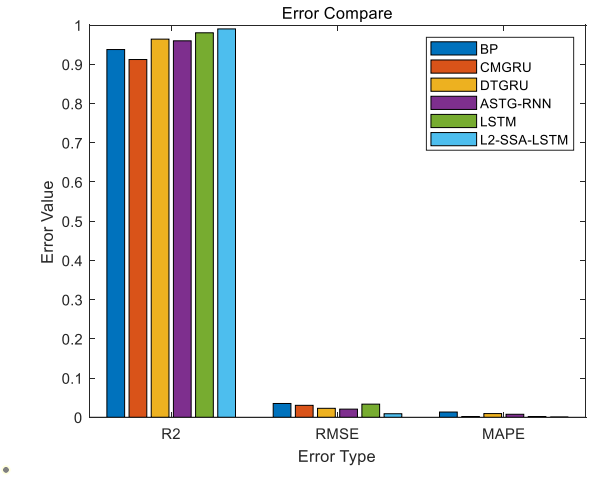

FIGURE 17. Prediction error results of various models.

As shown in Table 4 and Figure 14, the evaluation metrics RMSE and MAPE for the L2-SSA-LSTM prediction model are 0.00456 and 0.000239, respectively. Both RMSE and MAPE values are lower than those of other prediction

TABLE 5. Prediction error of different deviation angle models.

Prediction Model	R^2	RMSE	MAPE
BP	0.93771	0.03514	0.01333
CMGRU	0.91224	0.03042	0.00146
DTGRU	0.96423	0.02281	0.00938
ASTG-RNN	0.95993	0.02074	0.00762
LSTM	0.98039	0.03345	0.00157
L2-SSA-LSTM	0.99027	0.00892	0.000239

TABLE 6. Prediction error of different tool face angle models.

Prediction Model	R^2	RMSE	MAPE
BP	0.93985	0.20318	0.03245
CMGRU	0.98778	0.13234	0.01918
DTGRU	0.97239	0.11248	0.01326
ASTG-RNN	0.87383	0.18682	0.01077
LSTM	0.98742	0.13753	0.00314
L2-SSA-LSTM	0.99551	0.00822	0.00037

models, indicating that the L2-SSA-LSTM prediction model accurately predicts the target variable, with minimal differences between its predictions and the actual observed values. The R^2 evaluation metric for the L2-SSA-LSTM model is 0.99065, surpassing the R2 values of other models. This demonstrates that the L2-SSA-LSTM prediction model can explain a significant portion of the variance in the dependent variable, highlighting its strong fitting capability and ability to capture the variability in observed data. Overall, the L2-SSA-LSTM prediction model outperforms other models in terms of predictive accuracy.

5) DEVIATION ANGLE PREDICTION

From Figure 15, it is evident that when predicting the wellbore deviation angle, the various models exhibit significant differences in predictive performance for well depths between 2900 meters and 3000 meters and between 3100 meters and 3200 meters. However, the differences in predictive performance are minimal for other well depths. Overall, the L2-SSA-LSTM model outperforms other models in predicting the wellbore deviation angle, showing better predictive accuracy. As shown in Figure 16, the prediction errors for the bp model are generally within the range of $-0.1°$ to $0.06°$, for the CMGRU model within $-0.15°$ TO $0.06°$, for the DTGRU model within $-0.3°$ to $0.07°$, for the ASTG-RNN model within $-0.15°$ to $0.07°$, for the LSTM model within $-0.07°$to $0.15°$, and for the L2-SSA-LSTM model within approximately $\pm 0.07°$, demonstrating superior predictive performance.

By examining Table 5 and Figure 17, it can be observed that the evaluation metrics RMSE and MAPE for the L2-SSA-LSTM prediction model are measured at 0.00892 and 0.000239, respectively. These values are lower than the corresponding metrics for other prediction models, indicating minimal differences between the predictions of

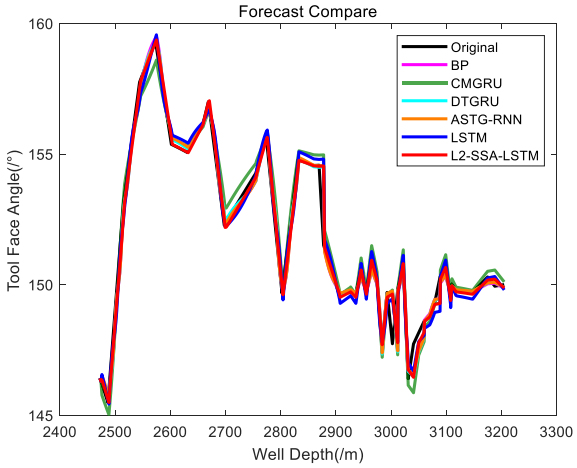

FIGURE 18. Tool face angle prediction results of various models.

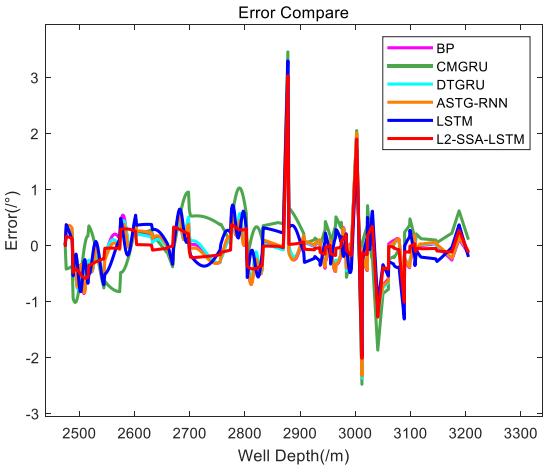

FIGURE 19. Prediction error results of various models.

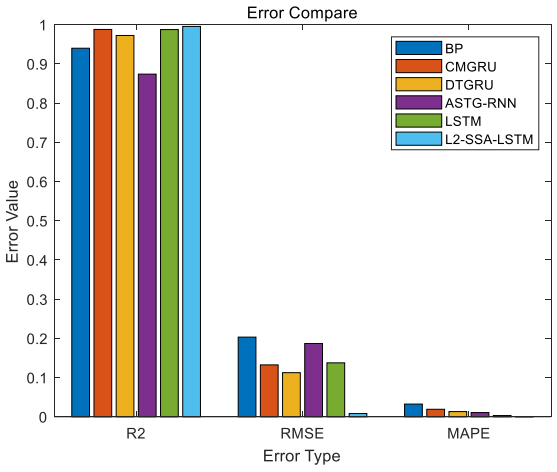

FIGURE 20. Prediction error results of various models.

the L2-SSA-LSTM model and the actual observed values, ultimately resulting in superior predictive performance compared to other models. The R^2 evaluation metric for the L2-SSA-LSTM model is 0.99027, surpassing the R^2 values

for other models. This highlights the strong fitting and predictive capabilities of the L2-SSA-LSTM prediction model in predicting the wellbore deviation angle. In the context of wellbore deviation angle prediction, the L2-SSA-LSTM prediction model demonstrates higher predictive accuracy and enhanced generalization capability, outperforming other models.

6) TOOL FACE ANGLE PREDICTION

From Figure 18, it is evident that when predicting the tool face angle, the CMGRU prediction model lags behind other models in terms of predictive performance. The BP, DTGRU, ASTG-RNN, and LSTM models show relatively small differences in their predictive effects but compared to the L2-SSA-LSTM model, their predictive performance is not as satisfactory. By observing the model prediction error plot in Figure 19, it can be seen that the prediction errors of the CMGRU model are roughly within the ±3°range, while the prediction errors of the BP, DTGRU, ASTG-RNN, and LSTM models are generally within the ±3.2°range. In contrast, the L2-SSA-LSTM prediction model achieves smaller prediction errors, typically within the ±2.9°range. This indicates that the L2-SSA-LSTM model exhibits superior predictive performance compared to other models.

By analyzing Table 6 and Figure 20, it can be observed that the evaluation metrics RMSE and MAPE for the L2-SSA-LSTM prediction model are recorded at 0.00822 and 0.00037. These values are significantly lower than the corresponding metrics for other prediction models, clearly reflecting the L2-SSA-LSTM model's effective capability to predict the target variable. The R2 evaluation metric for the L2-SSA-LSTM model is 0.99551, surpassing the R2 values for other models. This indicates that the L2-SSA-LSTM prediction model achieves a higher level of accuracy in tool face angle prediction, demonstrating superior predictive performance compared to other models.

V. CONCLUSION

The wellbore trajectory is a time series data. Starting from the time series of measuring the wellbore trajectory, the long short-term memory LSTM network prediction model is used to predict the azimuth angle, deviation angle, and tool face angle of the wellbore trajectory. Because the LSTM model has the problems of difficult adjustment of hyperparameters and easy over-fitting of the model, the sparrow algorithm SSA is used to optimize the hyperparameters of the LSTM network model, and L2 regularization is used to prevent the over-fitting of the LSTM network model. Therefore, the L2-SSA-LSTM model is constructed to predict and compare the azimuth angle, deviation angle, and tool face angle of the wellbore trajectory. The results show that the prediction results of the LSTM network model optimized by sparrow algorithm SSA and L2 regularization are more accurate than those of a single LSTM network, which provides a new method and theoretical basis for wellbore trajectory control technology, improves drilling efficiency and reduces drilling cost. The method proposed in this paper has yielded satisfactory predictive results; however, it has not yet been applied in practical drilling operations. In the future, we will continuously improve the method and apply it in real drilling activities. Furthermore, in subsequent research, we will consider expanding the model by means such as dataset storage and model optimization to enhance and extend the existing model's capability in handling more drilling data and real-time predictions, meeting the growing demands in the field of petroleum engineering.

REFERENCES

[1] M. R. Zare-Reisabadi, A. Kaffash, and S. R. Shadizadeh, "Determination of optimal well trajectory during drilling and production based on borehole stability," *Int. J. Rock Mech. Mining Sci.*, vol. 56, pp. 77–87, Dec. 2012, doi: 10.1016/j.ijrmms.2012.07.018.

[2] S. Costa, S. Stuckenbruck, A. B. Fontoura, and A. L. Martins, "Simulation of transient cuttings transportation and ECD in wellbore drilling," in *Proc. Europec/EAGE Conf. Exhib.*, vol. 10, Jun. 2008, pp. 9–12, doi: 10.2118/113893-MS.

[3] Y. Gao, F. Li, and J. Chen, "Random weighting adaptive estimation of model errors on attitude measurement for rotary steerable system," *IEEE Access*, vol. 10, pp. 80794–80803, 2022, doi: 10.1109/ACCESS.2022.3195519.

[4] M. Al-Rubaii, M. Al-Shargabi, D. Al-Shehri, A. Alyami, and K. M. Minaev, "A novel efficient borehole cleaning model for optimizing drilling performance in real time," *Appl. Sci.*, vol. 13, no. 13, p. 7751, Jun. 2023, doi: 10.3390/app13137751.

[5] A. Nautiyal and A. K. Mishra, "Drilling efficiency enhancement in oil and gas domain using machine learning," *Int. J. Oil, Gas Coal Technol.*, vol. 32, no. 4, p. 340, Feb. 2023, doi: 10.1504/IJOGCT.2023.129577.

[6] M. J. Bailey, S. L. Roberts, A. Suleiman, and A. Ismail, "Deployment of an eccentric borehole conditioning tool yields significant drilling efficiency improvements," *Middle East Oil*, vol. 13, no. 6, pp. 19–21, Mar. 2023, doi: https://doi.org/10.2118/213634-MS.

[7] H Li, X Wang, X Bai, Y Zhang, and Z Li, "A transient wellbore trajectory prediction model using transfer matrix method," *Int. J. Petroleum Petrochemical Eng.*, vol. 5, no. 3, pp. 52–60, Feb. 2019, doi: 10.20431/2454-7980.0503004.

[8] L. Yang, J. Tian, Q. Liu, L. Dai, Z. Hu, and J. Li, "The multidirectional vibration and coupling dynamics of drill string and its influence on the wellbore trajectory," *J. Mech. Sci. Technol.*, vol. 34, no. 7, pp. 2681–2692, Jul. 2020, doi: 10.1007/s12206-020-0601-x.

[9] X. Xie, Y. Tang, and H. Xu, "Prediction method for wellbore trajectory in horizontal drilling sections," *J. China Univ. Petroleum Ed. Natural Sci.*, vol. 36, no. 4, pp. 62–76, Dec. 2022, doi: 10.3969/j.issn.1673-5935.2022.04.011.

[10] R. Samuel and S. Zhang, "Geometrically and mechanically coupled borehole energy based project ahead model for real time well engineering," in *Proc. SPE/IADC Middle East Drilling Technol. Conf. Exhib.*, vol. 10, no. 2, May 2023, pp. 23–42, doi: 10.2118/214630-MS.

[11] B. Yan, X. Zhang, C. Tang, X. Wang, Y. Yang, and W. Xu, "A random forest-based method for predicting borehole trajectories," *Mathematics*, vol. 11, no. 6, p. 1297, Mar. 2023, doi: 10.3390/math11061297.

[12] R. W. Liu, K. Hu, M. Liang, Y. Li, X. Liu, and D. Yang, "QSD-LSTM: Vessel trajectory prediction using long short-term memory with quaternion ship domain," *Appl. Ocean Res.*, vol. 136, Jul. 2023, Art. no. 103592, doi: 10.1016/j.apor.2023.103592.

[13] F. Hasan and H. Huang, "MALS-Net: A multi-head attention-based LSTM sequence-to-sequence network for socio-temporal interaction modelling and trajectory prediction," *Sensors*, vol. 23, no. 1, p. 530, Jan. 2023, doi: 10.3390/s23010530.

[14] Y. Wang, J. Wang, J. Jiang, S. Xu, and J. Wang, "SA-LSTM: A trajectory prediction model for complex off-road multi-agent systems considering situation awareness based on risk field," *IEEE Trans. Veh. Technol.*, to be published, doi: 10.1109/TVT.2023.3287227.

[15] J. Zhang, H. Wang, F. Cui, Y. Liu, Z. Liu, and J. Dong, "Research into ship trajectory prediction based on an improved LSTM network," *J. Mar. Sci. Eng.*, vol. 11, no. 7, p. 1268, Jun. 2023, doi: 10.3390/jmse11071268.

[16] Y. Qin, J. Zhou, D. Xiao, C. Qin, and Q. Qian, "High-precision cutterhead torque prediction for tunnel boring machines using an attention-based embedded LSTM neural network," *Measurement*, vol. 224, Jan. 2024, Art. no. 113888, doi: 10.1016/j.measurement.2023.113888.
[17] J. Zhou, Y. Qin, J. Luo, S. Wang, and T. Zhu, "Dual-thread gated recurrent unit for gear remaining useful life prediction," *IEEE Trans. Ind. Informat.*, vol. 19, no. 7, pp. 8307–8318, Jul. 2023, doi: 10.1109/TII.2022.3217758.
[18] J. Zhou, Y. Qin, J. Luo, and T. Zhu, "Remaining useful life prediction by distribution contact ratio health indicator and consolidated memory GRU," *IEEE Trans. Ind. Informat.*, vol. 19, no. 7, pp. 8472–8483, Jul. 2023, doi: 10.1109/TII.2022.3218665.
[19] M. Huang, K. Zhou, L. Wang, and J. Zhou, "Application of long short-term memory network for wellbore trajectory prediction," *Petroleum Sci. Technol.*, vol. 2, pp. 29–35, Dec. 2023, doi: 10.1080/10916466.2023.2193608.
[20] Y. Bai, S. Xiang, F. Cheng, and J. Zhao, "A dynamic-inner LSTM prediction method for key alarm variables forecasting in chemical process," *Chin. J. Chem. Eng.*, vol. 55, pp. 266–276, Mar. 2023, doi: 10.1016/j.cjche.2022.08.024.
[21] M. Yuan, Z. Li, C. Zhang, L. Zheng, K. Mao, and F. Pei, "Research on real-time prediction of completion time based on AE-CNN-LSTM," *Comput. Ind. Eng.*, vol. 185, Nov. 2023, Art. no. 109677, doi: 10.1016/j.cie.2023.109677.
[22] P. Redhu and K. Kumar, "Short-term traffic flow prediction based on optimized deep learning neural network: PSO-Bi-LSTM," *Phys. A, Stat. Mech. Appl.*, vol. 625, Sep. 2023, Art. no. 129001, doi: 10.1016/j.physa.2023.129001.
[23] B. Usharani, *ILF-LSTM: Enhanced Loss Function in LSTM to Predict the sea Surface Temperature*, vol. 27. Cham, Switzerland: Springer, Mar. 2023, pp. 13129–13141, doi: 10.1007/s00500-022-06899-y.
[24] C. Zhang and S. Ding, "A stochastic configuration network based on chaotic sparrow search algorithm," *Knowl.-Based Syst.*, vol. 220, May 2021, Art. no. 106924, doi: 10.1016/j.knosys.2021.106924.
[25] B. Gao, W. Shen, H. Guan, L. Zheng, and W. Zhang, "Research on multistrategy improved evolutionary sparrow search algorithm and its application," *IEEE Access*, vol. 10, pp. 62520–62534, 2022, doi: 10.1109/ACCESS.2022.3182241.
[26] C. Zhang, P. Chen, F. Jiang, J. Xie, and T. Yu, "Fault diagnosis of nuclear power plant based on sparrow search algorithm optimized CNN-LSTM neural network," *Energies*, vol. 16, no. 6, p. 2934, Mar. 2023, doi: 10.3390/en16062934.
[27] K. Meng, C. Chen, and B. Xin, "MSA: A multi-strategy enhanced sparrow search algorithm for global optimization problems," *Frontiers Inf. Technol. Electron. Eng.*, vol. 23, pp. 1828–1848, Dec. 2022, doi: 10.1631/FITEE.2200237.

YI GAO received the B.S. degree in automation control, the M.S. degree in control theory and control engineering, and the Ph.D. degree in traffic information engineering and control from Northwestern Polytechnical University, Xi'an, China, in 2002 and 2008, respectively. Since 2014, she has been an Associate Professor with Xi'an Shiyou University. She is the author of two books, more than 30 articles, and ten inventions. Her research interests include drilling automation technology, attitude measurement, and intelligent control.

NA WANG received the bachelor's degree from Xi'an Shiyou University, in 2022. She is currently pursuing the Graduate degree. Her research interest includes wellbore trajectory prediction.

YIHAO MA received the bachelor's degree from Xi'an Shiyou University, in 2022. He is currently pursuing the Graduate degree. His research interest includes motor fault diagnose.